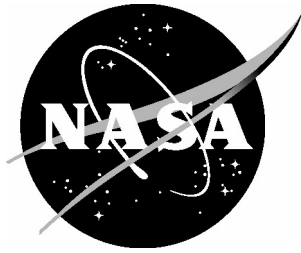


NASA/TM-2004-213251



Instrument Attitude Precision Control

Jer-Nan Juang
Langley Research Center, Hampton, Virginia

August 2004

The NASA STI Program Office . . . in Profile

Since its founding, NASA has been dedicated to the advancement of aeronautics and space science. The NASA Scientific and Technical Information (STI) Program Office plays a key part in helping NASA maintain this important role.

The NASA STI Program Office is operated by Langley Research Center, the lead center for NASA's scientific and technical information. The NASA STI Program Office provides access to the NASA STI Database, the largest collection of aeronautical and space science STI in the world. The Program Office is also NASA's institutional mechanism for disseminating the results of its research and development activities. These results are published by NASA in the NASA STI Report Series, which includes the following report types:

- **TECHNICAL PUBLICATION.** Reports of completed research or a major significant phase of research that present the results of NASA programs and include extensive data or theoretical analysis. Includes compilations of significant scientific and technical data and information deemed to be of continuing reference value. NASA counterpart of peer-reviewed formal professional papers, but having less stringent limitations on manuscript length and extent of graphic presentations.
- **TECHNICAL MEMORANDUM.** Scientific and technical findings that are preliminary or of specialized interest, e.g., quick release reports, working papers, and bibliographies that contain minimal annotation. Does not contain extensive analysis.
- **CONTRACTOR REPORT.** Scientific and technical findings by NASA-sponsored contractors and grantees.

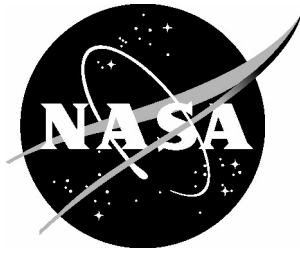
- **CONFERENCE PUBLICATION.** Collected papers from scientific and technical conferences, symposia, seminars, or other meetings sponsored or co-sponsored by NASA.
- **SPECIAL PUBLICATION.** Scientific, technical, or historical information from NASA programs, projects, and missions, often concerned with subjects having substantial public interest.
- **TECHNICAL TRANSLATION.** English-language translations of foreign scientific and technical material pertinent to NASA's mission.

Specialized services that complement the STI Program Office's diverse offerings include creating custom thesauri, building customized databases, organizing and publishing research results ... even providing videos.

For more information about the NASA STI Program Office, see the following:

- Access the NASA STI Program Home Page at <http://www.sti.nasa.gov>
- E-mail your question via the Internet to help@sti.nasa.gov
- Fax your question to the NASA STI Help Desk at (301) 621-0134
- Phone the NASA STI Help Desk at (301) 621-0390
- Write to:
NASA STI Help Desk
NASA Center for AeroSpace Information
7121 Standard Drive
Hanover, MD 21076-1320

NASA/TM-2004-213251



Instrument Attitude Precision Control

Jer-Nan Juang
Langley Research Center, Hampton, Virginia

National Aeronautics and
Space Administration

Langley Research Center
Hampton, Virginia 23681-2199

August 2004

Available from:

NASA Center for AeroSpace Information (CASI)
7121 Standard Drive
Hanover, MD 21076-1320
(301) 621-0390

National Technical Information Service (NTIS)
5285 Port Royal Road
Springfield, VA 22161-2171
(703) 605-6000

Instrument Attitude Precision Control

Jer-Nan Juang

NASA Langley Research Center

Hampton, VA 23681

Abstract

A novel approach is presented in this paper to analyze attitude precision and control for an instrument gimbaled to a spacecraft subject to an internal disturbance caused by a moving component inside the instrument. Nonlinear differential equations of motion for some sample cases are derived and solved analytically to gain insight into the influence of the disturbance on the attitude pointing error. A simple control law is developed to eliminate the instrument pointing error caused by the internal disturbance. Several cases are presented to demonstrate and verify the concept presented in this paper.

Keywords: Attitude dynamics and control, feedback control, spacecraft dynamics

Introduction

This paper was originally motivated by developing a fine-pointing control algorithm for enabling the GIFTS (Geostationary Imaging Fourier Transform Spectrometer) instrument to meet its mission requirements [1]. GIFTS combines a number of advanced technologies to observe atmospheric weather and chemistry variables in four dimensions. It will enable meteorological soundings equivalent to those achieved by simultaneously launching of 16,384 closely spaced radiosonde balloons within a 600-km diameter circle about every 10 seconds. It will revolutionize atmospheric science and meteorological forecasting. GIFTS instrument/mission affords an opportunity to space-qualify a significant number of new technologies, payload and non-payload specific, for future generation remote sensors.

The GIFTS attitude precision for the instrument pointing requires the use of a lightweight, low power, inexpensive, and highly reliable mini-star-tracker for estimation of the spacecraft orientation. Note that star cameras are among the most attractive attitude sensors, because they provide three-axis attitude information with high accuracy. Considerable work has been done in developing the mini-star-tracker, along with attitude estimation algorithms producing significant achievements as documented in Refs. [2-10]. The main role of the mini-star-tracker that will be integrated into an Optical Pointing and Stabilization Control System (OPSC) is to achieve the GIFTS pointing requirements.

The goal of the OPSC is to orient and stabilize the GIFTS optical instrument with respect to the Earth. OPSC will scan the earth as well as the near-stellar region off the earth's horizon in a step-stare procedure. Imaging occurs during a ten second stare at a specific point on earth, followed by a step motion of one FOV to a new target within one second, covering the disc of the earth approximately every 15 minutes. OPSC will also stabilize the optical boresight against disturbance motions generated by the spacecraft that carries the GIFTS optical instrument.

The original strategy of the GIFTS OPSC is shown in Figure 1. The optical platform is mounted on a two-axis flex-pivot gimbal for boresight pointing control while vibration is reduced through a high bandwidth jitter control mirror. Attitude measurements are made by a dual star camera system and jitter is measured by an MEMS rate sensor integrated with the star cameras. Gimbal and jitter mirror angle measurements are made using high precision electro-optic sensors. A separate processor is used for system control.

This paper begins with a brief introduction of two-body dynamics. All differential equations of motion derived for many differential cases are based on the fundamental concept of two-body dynamics. A simple configuration of a rigid body with an internal moving part representing the GIFTS instrument rigidly attached to a spacecraft will be discussed. Parametric studies will be performed to understand how the moving part influences the overall system motion, in particular the inertial pointing. The other configuration to be studied consists of one rigid body (spacecraft) gimballed by another rigid body (instrument) with a moving part inside. Three rigid bodies are involved in this configuration making the case extremely complex in deriving equations

of motion for designing a control-torque law to meet the instrument attitude precision requirements. Furthermore, it is very difficult, if not impossible, in performing parametric studies for general cases. For simplicity, without losing generality, we will limit the parametric and numerical studies in one rotational axis.

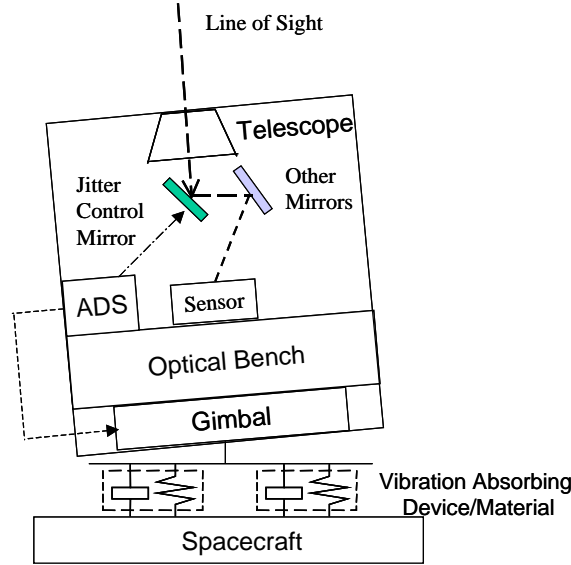


Figure 1: Optical Pointing and Stabilization Control System (OPSC).

Basic Formulation

The basic configuration consists of the spacecraft and the optical instrument with a moving mirror. OPSC is designed to orient and stabilize the optical instrument by providing a control torque/force against the spacecraft. During the control maneuvering, coupled motion of the spacecraft and the instrument takes place. To describe the overall system motion, multiple-body dynamics are involved. Basic formulations for two-body dynamics will be briefly described in this section [11].

From Figure 2, let m_a be the mass of the body a (for our case, the spacecraft that carries the optical instrument), \mathbf{v}_a be the velocity of the coordinate origin $\mathbf{0}_a$, $\boldsymbol{\omega}_a$ be the angular velocity of the body, and $\boldsymbol{\rho}_a$ be the distance vector from $\mathbf{0}_a$ to an arbitrary point

in the body. Subscript a signifies the associated quantity for the body. The linear momentum of the body over the domain Ω_a is described by

$$\mathbf{p}_a = \int_{\Omega_a} (\mathbf{v}_a + \boldsymbol{\omega}_a \times \mathbf{p}_a) dm_a = m_a (\mathbf{v}_a + \boldsymbol{\omega}_a \times \mathbf{c}_a) \quad (1)$$

where

$$\mathbf{c}_a = \frac{1}{m_a} \int_{\Omega_a} \mathbf{p}_a dm_a$$

is the definition of the center of mass (CM).

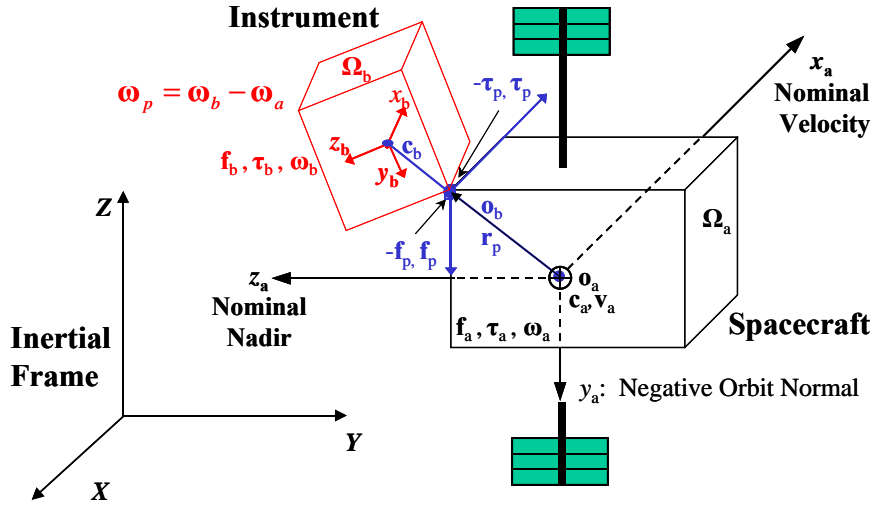


Figure 2: Body and inertia coordinates for two-body dynamics.

Similarly, define m_b as the mass of the body b , \mathbf{v}_b as the velocity of the coordinate origin \mathbf{o}_b , $\boldsymbol{\omega}_b$ as the angular velocity of the body b , \mathbf{r}_p as the distance vector from \mathbf{o}_a to \mathbf{o}_b where the optical instrument is maneuvered for fine pointing, and \mathbf{p}_b as the distance vector from \mathbf{o}_b to an arbitrary point in the body b . The linear momentum of the body b over the domain Ω_b is

$$\begin{aligned}
\mathbf{p}_b &= \int_{\Omega_b} [\mathbf{v}_b + \boldsymbol{\omega}_b \times \boldsymbol{\rho}_b] dm_b \\
&= \int_{\Omega_b} [\mathbf{v}_a + \boldsymbol{\omega}_a \times (\mathbf{r}_p + \boldsymbol{\rho}_b) + \boldsymbol{\omega}_p \times \boldsymbol{\rho}_b] dm_b \\
&= m_b [\mathbf{v}_a + \boldsymbol{\omega}_a \times (\mathbf{r}_p + \mathbf{c}_b) + \boldsymbol{\omega}_p \times \mathbf{c}_b]
\end{aligned} \tag{2}$$

where the angular velocity $\boldsymbol{\omega}_p$ of body b relative to body a is

$$\boldsymbol{\omega}_p = \boldsymbol{\omega}_b - \boldsymbol{\omega}_a$$

and the center of mass \mathbf{c}_b is

$$\mathbf{c}_b = \frac{1}{m_b} \int_{\Omega_b} \boldsymbol{\rho}_b dm_b$$

The basic momentum equation of motion about point $\mathbf{0}$ (a or b) is

$$\mathbf{h} = \int_{\Omega} \boldsymbol{\rho} \times (\mathbf{v}_o + \mathbf{v}) dm \tag{3}$$

with $\mathbf{v} = \dot{\boldsymbol{\rho}}$ being the velocity of an arbitrary point in Ω . Equation (3) is applicable for both bodies a and b . For body a , replace \mathbf{h} , $\boldsymbol{\rho}$, and \mathbf{v}_o by \mathbf{h}_a , $\boldsymbol{\rho}_a$, and \mathbf{v}_a . For body b , replace \mathbf{h} , $\boldsymbol{\rho}$, and \mathbf{v}_o by \mathbf{h}_b , $\boldsymbol{\rho}_b$, and \mathbf{v}_b . The angular momentum of the body a about its reference point $\mathbf{0}_a$ is

$$\mathbf{h}_a = \int_{\Omega_a} \boldsymbol{\rho}_a \times (\mathbf{v}_a + \boldsymbol{\omega}_a \times \boldsymbol{\rho}_a) dm_a = m_a (\mathbf{c}_a \times \mathbf{v}_a) + \mathbf{I}_a \boldsymbol{\omega}_a \tag{4}$$

where

$$\mathbf{I}_a \boldsymbol{\omega}_a = \int_{\Omega_a} \boldsymbol{\rho}_a \times (\boldsymbol{\omega}_a \times \boldsymbol{\rho}_a) dm_a = \left[\int_{\Omega_a} (\boldsymbol{\rho}_a^T \boldsymbol{\rho}_a \mathbf{1} - \boldsymbol{\rho}_a \boldsymbol{\rho}_a^T) dm_a \right] \boldsymbol{\omega}_a$$

and $\mathbf{1}$ is a 3 by 3 identity matrix. Note that the second equality is written in matrix form for easy numerical implementation. Similarly, The angular momentum of the body b about its reference point $\mathbf{0}_b$ is

$$\begin{aligned}
\mathbf{h}_b &= \int_{\Omega_b} \boldsymbol{\rho}_b \times (\mathbf{v}_b + \boldsymbol{\omega}_b \times \boldsymbol{\rho}_b) dm_b \\
&= \int_{\Omega_b} \boldsymbol{\rho}_b \times [\mathbf{v}_a + \boldsymbol{\omega}_a \times (\mathbf{r}_p + \boldsymbol{\rho}_b) + \boldsymbol{\omega}_p \times \boldsymbol{\rho}_b] dm_b \\
&= m_b (\mathbf{c}_b \times \mathbf{v}_a) + \mathbf{I}_{ba} \boldsymbol{\omega}_a + \mathbf{I}_b \boldsymbol{\omega}_p
\end{aligned} \tag{5}$$

where

$$\mathbf{I}_b \boldsymbol{\omega}_p = \int_{\Omega_b} \boldsymbol{\rho}_b \times (\boldsymbol{\omega}_p \times \boldsymbol{\rho}_b) dm_b = \left[\int_{\Omega_b} (\boldsymbol{\rho}_b^T \boldsymbol{\rho}_b \mathbf{1} - \boldsymbol{\rho}_b \boldsymbol{\rho}_b^T) dm_b \right] \boldsymbol{\omega}_p$$

and

$$\begin{aligned} \mathbf{I}_{ba} \boldsymbol{\omega}_a &= \int_{\Omega_b} \boldsymbol{\rho}_b \times [\boldsymbol{\omega}_a \times (\mathbf{r}_p + \boldsymbol{\rho}_b)] dm_b \\ &= \left[\int_{\Omega_b} [\boldsymbol{\rho}_b^T (\mathbf{r}_p + \boldsymbol{\rho}_b) \mathbf{1} - (\mathbf{r}_p + \boldsymbol{\rho}_b) \boldsymbol{\rho}_b^T] dm_b \right] \boldsymbol{\omega}_a \\ &= [\mathbf{I}_b + m_b (\mathbf{c}_b^T \mathbf{r}_p \mathbf{1} - \mathbf{r}_p \mathbf{c}_b^T)] \boldsymbol{\omega}_a \end{aligned}$$

The temporal derivative of \mathbf{h} from Eq. (3) becomes

$$\begin{aligned} \dot{\mathbf{h}} &= \int_{\Omega} \dot{\boldsymbol{\rho}} \times (\mathbf{v}_o + \mathbf{v}) dm + \int_{\Omega} \boldsymbol{\rho} \times (\dot{\mathbf{v}}_o + \dot{\mathbf{v}}) dm \\ &= \int_{\Omega} \mathbf{v} \times (\mathbf{v}_o + \mathbf{v}) dm + \int_{\Omega} \boldsymbol{\rho} \times d\mathbf{f} \\ &= \mathbf{p} \times \mathbf{v}_o + \boldsymbol{\tau} \end{aligned} \quad (6)$$

From Eqs. (1) and (2), the equations of motion for translation are:

$$\dot{\mathbf{p}}_a = \mathbf{f}_a - \mathbf{f}_p \quad (7)$$

and

$$\dot{\mathbf{p}}_b = \mathbf{f}_b + \mathbf{f}_p \quad (8)$$

where \mathbf{f}_a and \mathbf{f}_b are external forces applied to a and b respectively, and \mathbf{f}_p is the internal force acting at the joint $\mathbf{0}_b$. From Eq. (6), the equation of motion for rotation about the origin $\mathbf{0}_a$ for the body a is:

$$\dot{\mathbf{h}}_a + \mathbf{v}_a \times \mathbf{p}_a = \boldsymbol{\tau}_a - \boldsymbol{\tau}_p + \mathbf{r}_p \times \mathbf{f}_p \quad (9)$$

and the equation of motion for rotation about the joint $\mathbf{0}_b$ for the body b is

$$\dot{\mathbf{h}}_b + (\mathbf{v}_a + \boldsymbol{\omega}_a \times \mathbf{r}_p) \times \mathbf{p}_b = \boldsymbol{\tau}_b + \boldsymbol{\tau}_p \quad (10)$$

where $\boldsymbol{\tau}_a$ and $\boldsymbol{\tau}_b$ are external toques applied to a and b respectively, and $\boldsymbol{\tau}_p$ is the internal torque acting at $\mathbf{0}_b$.

Summing Eqs. (7) and (8) for system translation yields

$$\dot{\mathbf{p}}_a + \dot{\mathbf{p}}_b = \mathbf{f}_a + \mathbf{f}_b \Rightarrow \dot{\mathbf{p}} = \mathbf{f} \quad (11)$$

The rate of change in the total system momentum equals to the total external force. On the other hand, adding Eq. (9) to Eq. (10) for system rotation gives

$$\dot{\mathbf{h}} + \mathbf{v}_a \times \mathbf{p} = \boldsymbol{\tau} \quad (12)$$

where the total angular momentum

$$\mathbf{h} = \mathbf{h}_a + \mathbf{h}_b + \mathbf{r}_p \times \mathbf{p}_b = m(\mathbf{c} \times \mathbf{v}_a) + \mathbf{I}\boldsymbol{\omega}_a + \mathbf{I}_{ab}\boldsymbol{\omega}_p \quad (13)$$

and the torque is

$$\boldsymbol{\tau} = \boldsymbol{\tau}_a + \boldsymbol{\tau}_b + \mathbf{r}_p \times \mathbf{f}_b$$

The total moment of inertia over Ω_a and Ω_b about $\mathbf{0}_a$ is

$$\begin{aligned} \mathbf{I} &= \mathbf{I}_a + \int_{\Omega_b} [(\mathbf{r}_p + \boldsymbol{\rho}_b)^T (\mathbf{r}_p + \boldsymbol{\rho}_b) \mathbf{1} - (\mathbf{r}_p + \boldsymbol{\rho}_b)(\mathbf{r}_p + \boldsymbol{\rho}_b)^T] dm_b \\ &= \mathbf{I}_a + \mathbf{I}_b + m_b(\mathbf{r}_p^T \mathbf{r}_p \mathbf{1} - \mathbf{r}_p \mathbf{r}_p^T) + m_b(2\mathbf{r}_p^T \mathbf{c}_b \mathbf{1} - \mathbf{r}_p \mathbf{c}_b^T - \mathbf{c}_b \mathbf{r}_p^T) \end{aligned}$$

The center of mass for the whole system over Ω_a and Ω_b is

$$m\mathbf{c} = m_a \mathbf{c}_a + m_b(\mathbf{c}_b + \mathbf{r}_p); \quad m = m_a + m_b$$

The mix moment of inertia is

$$\mathbf{I}_{ab} = \int_{\Omega_b} [\boldsymbol{\rho}_b^T (\mathbf{r}_p + \boldsymbol{\rho}_b) \mathbf{1} - \boldsymbol{\rho}_b (\mathbf{r}_p + \boldsymbol{\rho}_b)^T] dm_b = \mathbf{I}_b + m_b(\mathbf{r}_p^T \mathbf{c}_b \mathbf{1} - \mathbf{c}_b \mathbf{r}_p^T)$$

Equation (12) implies that the rate of change in the total system angular momentum equals the total external torque. The equation of motion to orient and stabilize body b can be obtained by inserting Eq. (2) into Eq. (10) to yield

$$\dot{\mathbf{h}}_b = (\mathbf{v}_a + \boldsymbol{\omega}_a \times \mathbf{r}_p) \times [m_b \mathbf{c}_b \times (\boldsymbol{\omega}_a + \boldsymbol{\omega}_p)] + \boldsymbol{\tau}_b + \boldsymbol{\tau}_p \quad (14)$$

Equations (11), (12), and (14) are differential equations of motion for a two-body dynamical problem with one body to be reoriented for fine pointing. For easy numerical implementation, they may be reformulated in terms of matrix form as

$$\begin{aligned} \dot{\mathbf{p}} &= -[\boldsymbol{\omega}_a \times] \mathbf{p} - \mathbf{f} \\ \dot{\mathbf{h}} &= \boldsymbol{\tau} - [\boldsymbol{\omega}_a \times] \mathbf{h} - [\mathbf{v}_a \times] \mathbf{p} \\ \dot{\mathbf{h}}_b &= \left\{ [\mathbf{h}_b \times] + [\mathbf{T}_{ba}(\mathbf{v}_a + [\boldsymbol{\omega}_a \times] \mathbf{r}_p) \times] [m_b \mathbf{c}_b \times] \right\} (\mathbf{T}_{ba} \boldsymbol{\omega}_a + \boldsymbol{\omega}_p) + \boldsymbol{\tau}_b + \boldsymbol{\tau}_p \end{aligned} \quad (15)$$

where each vector quantity has three components, and \mathbf{T}_{ba} is the transformation matrix from the body frame a to the body frame b . For any vector $\boldsymbol{\omega}$, its $[\boldsymbol{\omega} \times]$ is

$$\boldsymbol{\omega} = \begin{Bmatrix} \omega_1 \\ \omega_2 \\ \omega_3 \end{Bmatrix} \Rightarrow [\boldsymbol{\omega} \times] = \begin{bmatrix} 0 & -\omega_3 & \omega_2 \\ \omega_3 & 0 & -\omega_1 \\ -\omega_2 & \omega_1 & 0 \end{bmatrix}$$

Based on Eqs. (1), (2), (5), and (13), the momentum equation in matrix form is

$$\wp = \mathbf{M} \mathbf{v} \Rightarrow \begin{bmatrix} \mathbf{p} \\ \mathbf{h} \\ \mathbf{h}_b \end{bmatrix} = \begin{bmatrix} m\mathbf{1} & -[m\mathbf{c}\times] & -\mathbf{T}_{ab}[m_b\mathbf{c}_b\times] \\ [m\mathbf{c}\times] & \mathbf{I} & \mathbf{I}_{ab} \\ [m_b\mathbf{c}_b\times]\mathbf{T}_{ba} & \mathbf{I}_{ba} & \mathbf{I}_b \end{bmatrix} \begin{bmatrix} \mathbf{v}_a \\ \boldsymbol{\omega}_a \\ \boldsymbol{\omega}_p \end{bmatrix} \quad (16)$$

where

$$\begin{aligned} \mathbf{c} &= \frac{1}{m} \left[m_a \mathbf{c}_a + m_b (\mathbf{T}_{ab} \mathbf{c}_b + \mathbf{r}_p) \right]; \quad m = m_a + m_b \\ \mathbf{I} &= \mathbf{I}_a + \mathbf{T}_{ab} \mathbf{I}_b \mathbf{T}_{ab}^T + m_b \left[(\mathbf{r}_p^T \mathbf{r}_p) \mathbf{1} - \mathbf{r}_p \mathbf{r}_p^T \right] + m_b \left[2(\mathbf{r}_p^T \mathbf{T}_{ab} \mathbf{c}_b) \mathbf{1} - \mathbf{r}_p \mathbf{c}_b^T \mathbf{T}_{ab}^T - \mathbf{T}_{ab} \mathbf{c}_b \mathbf{r}_p^T \right] \\ \mathbf{I}_{ab} &= \mathbf{T}_{ab} \left\{ \mathbf{I}_b + m_b \left[(\mathbf{c}_b^T \mathbf{T}_{ba} \mathbf{r}_p) \mathbf{1} - \mathbf{c}_b \mathbf{r}_p^T \mathbf{T}_{ba}^T \right] \right\} \\ \mathbf{I}_{ba} &= \left\{ \mathbf{I}_b + m_b \left[(\mathbf{c}_b^T \mathbf{T}_{ba} \mathbf{r}_p) \mathbf{1} - \mathbf{T}_{ba} \mathbf{r}_p \mathbf{c}_b^T \right] \right\} \mathbf{T}_{ba} \end{aligned}$$

Note that \mathbf{p} and \mathbf{h} contain components in the body frame a , but \mathbf{h}_b contains components in the body frame b . Angular velocity becomes

$$\mathbf{v} = \mathbf{M}^{-1} \wp \quad (17)$$

To compute the transformation matrix from one frame to the other involves kinematics. Let the quaternion vector \mathbf{q} be the four components expressed by

$$\mathbf{q} = \begin{bmatrix} q_1 \\ q_2 \\ q_3 \\ q_4 \end{bmatrix} \quad (18)$$

The quaternion vector equation is

$$\frac{d}{dt} \mathbf{q} = \frac{1}{2} (q_4 \boldsymbol{\omega} - \boldsymbol{\omega} \times \mathbf{q}) \quad (19)$$

and its scalar equation is

$$\frac{d}{dt} q_4 = -\frac{1}{2} \boldsymbol{\omega} \cdot \mathbf{q} \quad (20)$$

Equations (19) and (20) in matrix form are

$$\begin{bmatrix} \dot{q}_1 \\ \dot{q}_2 \\ \dot{q}_3 \\ \dot{q}_4 \end{bmatrix} = \frac{1}{2} \begin{bmatrix} 0 & \omega_3 & -\omega_2 & \omega_1 \\ -\omega_3 & 0 & \omega_1 & \omega_2 \\ \omega_2 & -\omega_1 & 0 & \omega_3 \\ -\omega_1 & -\omega_2 & -\omega_3 & 0 \end{bmatrix} \begin{bmatrix} q_1 \\ q_2 \\ q_3 \\ q_4 \end{bmatrix} \quad (21)$$

Note that both bodies have the same form of kinematics. For the spacecraft, replace ω by ω_a and \mathbf{q} by \mathbf{q}_a . For the instrument, replace ω by ω_b and \mathbf{q} by \mathbf{q}_b . The transformation matrix from inertia frame to body frame becomes

$$\mathbf{T}_{\text{BI}} = \begin{bmatrix} q_1^2 - q_2^2 - q_3^2 + q_4^2 & 2(q_1 q_2 + q_4 q_3) & 2(q_1 q_3 - q_4 q_2) \\ 2(q_2 q_1 - q_4 q_3) & -q_1^2 + q_2^2 - q_3^2 + q_4^2 & 2(q_2 q_3 + q_4 q_1) \\ 2(q_3 q_1 + q_4 q_2) & 2(q_3 q_2 - q_4 q_1) & -q_1^2 - q_2^2 + q_3^2 + q_4^2 \end{bmatrix} \quad (22)$$

This matrix and its transpose are used to transform vectors from the inertia frame to the body frame, and vice versa.

One-Rotation-Axis Plane Motion

For simplicity, let us assume that the moving mirror is the only moving part of the spacecraft together with the optical instrument. In other words, the optical instrument is locked to the spacecraft as shown in Figure 3.

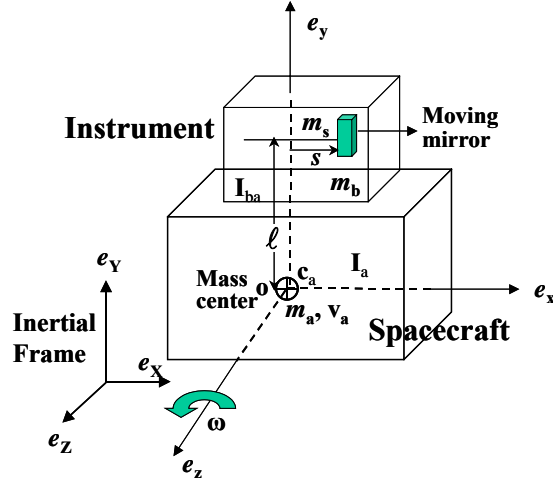


Figure 3: Body and inertia coordinates for one-rotation-axis plane motion.

The spacecraft linear momentum with the total mass m_a and the coordinate origin at the center of mass is

$$\begin{aligned} \mathbf{p}_a &= m_a \mathbf{v}_a = m_a (\dot{X} \mathbf{e}_x + \dot{Y} \mathbf{e}_y) \\ &= m_a (\dot{X} \cos \theta + \dot{Y} \sin \theta) \mathbf{e}_x + m_a (-\dot{X} \sin \theta + \dot{Y} \cos \theta) \mathbf{e}_y \end{aligned} \quad (23)$$

where θ is the rotation angle from the inertia frame and the body frame. The unit vector \mathbf{e}_x indicates the direction of the inertia axis X , and \mathbf{e}_y is the unit vector for the inertia axis Y . The quantities \dot{X} and \dot{Y} are the speeds of the coordinate origin along \mathbf{e}_x and \mathbf{e}_y , respectively. The instrument linear momentum with the mass m_b is

$$\begin{aligned}\mathbf{p}_b &= m_b \left[\mathbf{v}_a + \boldsymbol{\omega}_a \times (\mathbf{r}_p + \mathbf{c}_b) \right] = m_b [(\dot{X}\mathbf{e}_x + \dot{Y}\mathbf{e}_y) + \dot{\theta}\mathbf{e}_z \times \ell\mathbf{e}_y] \\ &= m_b [(\dot{X} \cos \theta + \dot{Y} \sin \theta - \ell \dot{\theta})\mathbf{e}_x + (-\dot{X} \sin \theta + \dot{Y} \cos \theta)\mathbf{e}_y]\end{aligned}\quad (24)$$

where the unit vectors \mathbf{e}_x , \mathbf{e}_y , and \mathbf{e}_z give the directions of the body coordinates x , y , and z , respectively. The quantity $\dot{\theta}$ is the angular velocity of the spacecraft, and ℓ is the distance from the center of mass of the spacecraft to the center of mass of the instrument. The moving-mirror linear momentum (assume point mass) is

$$\begin{aligned}\mathbf{p}_s &= m_s (\mathbf{v}_a + \boldsymbol{\omega}_a \times \mathbf{r}_s + \dot{\mathbf{s}}) = m_s [(\dot{X}\mathbf{e}_x + \dot{Y}\mathbf{e}_y) + \dot{\theta}\mathbf{e}_z \times (\ell\mathbf{e}_y + s\mathbf{e}_x) + \dot{s}\mathbf{e}_x] \\ &= m_s [(\dot{X} \cos \theta + \dot{Y} \sin \theta - \ell \dot{\theta} + \dot{s})\mathbf{e}_x + (-\dot{X} \sin \theta + \dot{Y} \cos \theta + s\dot{\theta})\mathbf{e}_y]\end{aligned}\quad (25)$$

where s is the distance from the center of mass of the instrument to the moving-mirror that is considered as a point mass..

Note the following coordinate transformation

$$\begin{cases} \dot{x} = \dot{X} \cos \theta + \dot{Y} \sin \theta \\ \dot{y} = -\dot{X} \sin \theta + \dot{Y} \cos \theta \end{cases}\quad (26)$$

Equations (23), (24), and (26) reduce to

$$\begin{aligned}\mathbf{p}_a &= m_a [\dot{x}\mathbf{e}_x + \dot{y}\mathbf{e}_y] \\ \mathbf{p}_b &= m_b [(\dot{x} - \ell \dot{\theta})\mathbf{e}_x + \dot{y}\mathbf{e}_y] \\ \mathbf{p}_s &= m_s [(\dot{x} - \ell \dot{\theta} + \dot{s})\mathbf{e}_x + (\dot{y} + s\dot{\theta})\mathbf{e}_y]\end{aligned}\quad (27)$$

Spacecraft angular momentum about the reference point \mathbf{o} is

$$\mathbf{h}_a = \int_{\Omega_a} \boldsymbol{\rho}_a \times (\mathbf{v}_a + \boldsymbol{\omega}_a \times \boldsymbol{\rho}_a) dm_a = \mathbf{I}_a \boldsymbol{\omega}_a = \mathbf{I}_a \dot{\theta} \mathbf{e}_z \quad (28)$$

Instrument angular momentum about the reference point \mathbf{o} is

$$\begin{aligned}
\mathbf{h}_b &= m_b \mathbf{c}_b \times \mathbf{v}_a + \mathbf{I}_{ba} \boldsymbol{\omega}_a \\
&= m_b \ell \mathbf{e}_y \times [\dot{x} \mathbf{e}_x + \dot{y} \mathbf{e}_y] + \mathbf{I}_{ba} \dot{\theta} \mathbf{e}_z \\
&= [-m_b \ell \dot{x} + \mathbf{I}_{ba} \dot{\theta}] \mathbf{e}_z
\end{aligned} \tag{29}$$

Moving-mirror angular momentum about the reference point \mathbf{o} is

$$\begin{aligned}
\mathbf{h}_s &= m_s [\mathbf{r}_s \times (\mathbf{v}_a + \boldsymbol{\omega}_a \times \mathbf{r}_s + \dot{\mathbf{r}}_s)] \\
&= m_s [\ell \mathbf{e}_y + s \mathbf{e}_x] \times \left\{ [\dot{x} - \ell \dot{\theta} + \dot{s}] \mathbf{e}_x + [\dot{y} + s \dot{\theta}] \mathbf{e}_y \right\} \\
&= m_s \{ -\ell [\dot{x} - \ell \dot{\theta} + \dot{s}] + s [\dot{y} + s \dot{\theta}] \} \mathbf{e}_z
\end{aligned} \tag{30}$$

Translational equation of motion for the whole system is

$$\mathbf{p} = \mathbf{p}_a + \mathbf{p}_b + \mathbf{p}_s = \mathbf{0} \Rightarrow \begin{cases} (m_a + m_b + m_s) \dot{x} - (m_b + m_s) \ell \dot{\theta} = -m_s \dot{s} \\ (m_a + m_b + m_s) \dot{y} + m_s s \dot{\theta} = 0 \end{cases} \tag{31}$$

Rotational equation of motion for the whole system with $\mathbf{p} = \mathbf{0}$ is

$$\begin{aligned}
\mathbf{h} &= \mathbf{h}_a + \mathbf{h}_b + \mathbf{h}_s = \mathbf{0} \\
&\Rightarrow -(m_b + m_s) \ell \dot{x} + m_s s \dot{y} + [\mathbf{I}_a + \mathbf{I}_{ba} + m_s (\ell^2 + s^2)] \dot{\theta} = m_s \ell \dot{s}
\end{aligned} \tag{32}$$

Equations (31) and (32) yield the following matrix equation of motion

$$\begin{bmatrix} m_a + m_b + m_s & 0 & -(m_b + m_s) \ell \\ 0 & m_a + m_b + m_s & m_s s \\ -(m_b + m_s) \ell & m_s s & \mathbf{I}_a + \mathbf{I}_{ba} + m_s (\ell^2 + s^2) \end{bmatrix} \begin{bmatrix} \dot{x} \\ \dot{y} \\ \dot{\theta} \end{bmatrix} = \begin{bmatrix} -m_s \dot{s} \\ 0 \\ m_s \ell \dot{s} \end{bmatrix} \tag{33}$$

Define the non-dimensional quantities as

$$\begin{aligned}
\bar{x} &= \frac{x}{\ell}, \quad \bar{y} = \frac{y}{\ell}, \quad \bar{s} = \frac{s}{\ell}, \\
m_1 &= \frac{m_b + m_s}{m_a + m_b + m_s}, \quad m_2 = \frac{m_s}{m_a + m_b + m_s} \\
\mathbf{I}_1 &= \frac{\mathbf{I}_a + \mathbf{I}_{ba} + m_s \ell^2}{(m_a + m_b + m_s) \ell^2}
\end{aligned} \tag{34}$$

then the matrix equation of motion, i.e., Eq. (33), becomes

$$\begin{bmatrix} 1 & 0 & -m_1 \\ 0 & 1 & m_2 \bar{s} \\ -m_1 & m_2 \bar{s} & \mathbf{I}_1 + m_2 \bar{s}^2 \end{bmatrix} \begin{bmatrix} \dot{\bar{x}} \\ \dot{\bar{y}} \\ \dot{\theta} \end{bmatrix} = \begin{bmatrix} -m_2 \dot{\bar{s}} \\ 0 \\ m_2 \dot{\bar{s}} \end{bmatrix} \tag{35}$$

Equation (35) may be solved to yield the following differential equations to be integrated

$$\dot{\bar{x}} = \frac{-m_2 \left[I_1 - m_1 + (1 - m_2) m_2 \bar{s}^2 \right] \dot{\bar{s}}}{I_1 - m_1^2 + (1 - m_2) m_2 \bar{s}^2} \quad (36)$$

$$\dot{\bar{y}} = \frac{-(1 - m_1) m_2^2 \dot{\bar{s}}}{I_1 - m_1^2 + (1 - m_2) m_2 \bar{s}^2} \quad (37)$$

$$\dot{\theta} = \frac{-(1 - m_1) m_2 \dot{\bar{s}}}{I_1 - m_1^2 + (1 - m_2) m_2 \bar{s}^2} \quad (38)$$

Analytical solutions for Eqs. (36), (37), and (38) are

$$\theta = \frac{(1 - m_1) \tan^{-1} \left[\bar{s} \sqrt{(1 - m_2) m_2 / (I_1 - m_1^2)} \right]}{\sqrt{(I_1 - m_1^2) (1 - m_2) / m_2}} \quad (39)$$

$$\bar{y} = -\frac{(1 - m_1) m_2 \log \left[I_1 - m_1^2 + (1 - m_2) m_2 \bar{s}^2 \right]}{2(1 - m_2)} \quad (40)$$

and

$$\bar{x} = m_1 \theta - m_2 \bar{s} \quad (41)$$

Equation (39) shows the relationship among the rotation angle θ , the moving-mirror motion \bar{s} , and the inertia ratio I_1 with given mass ratios m_1 and m_2 . The angle error θ induced by the moving-mirror motion is proportional to \bar{s} for sufficiently small \bar{s} and large I_1 , because under such condition $\tan^{-1} \left[\bar{s} \sqrt{(1 - m_2) m_2 / (I_1 - m_1^2)} \right]$ approaches

$\bar{s} \sqrt{(1 - m_2) m_2 / (I_1 - m_1^2)}$. Figure 4 illustrates the complex but interesting relationship

where the moving mass, the spacecraft mass, and the instrument mass were given from an earlier GIFTS design. For large moving-mirror motion ($\bar{s} \rightarrow 1$) and relatively small inertia ratio ($I_1 < 20$), the pointing-angle error may be larger than 0.02 degree. The inequality $I_1 < 20$ implies that the moving mirror is located away from the center of mass of the spacecraft ($\ell \gg 0$) and the moment of inertia ($I_a + I_{ba} + m_s \ell^2$) is relatively small such that the ratio of $I_a + I_{ba} + m_s \ell^2$ to $(m_a + m_b + m_s) \ell^2$ is less than 20. The relationship surface is quite nonlinear in the upper-front-end corner. To minimize the pointing-angle error via a control torque requires a nonlinear control law that will be developed in the following section.

Moving-mirror mass $m_s = 10$ Kg
Spacecraft mass $m_a = 726$ Kg
Instrument mass $m_b = 190$ Kg

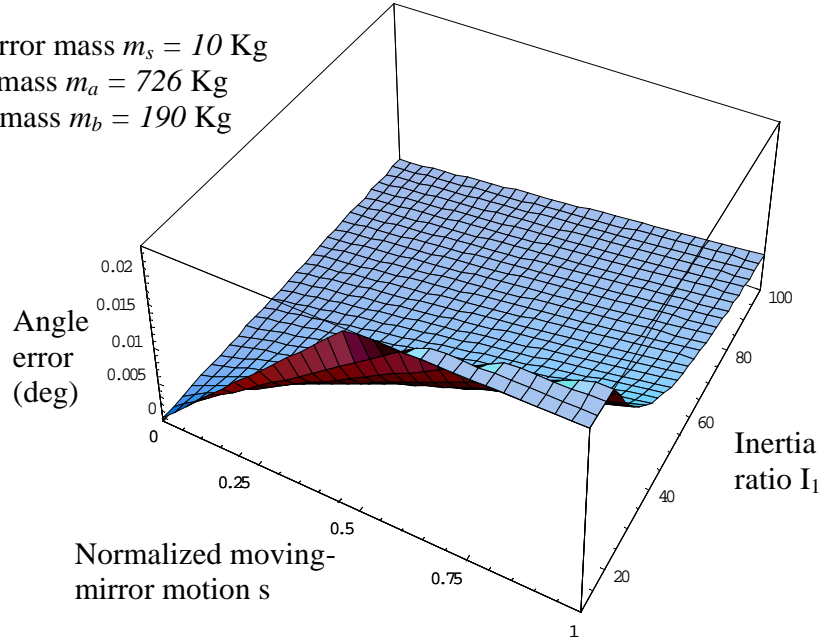


Figure 4: Relationship among the angle error θ , the moving-mirror motion \bar{s} , and the inertia ratio I_1 .

Two-Rotation-Axis Plane Motion

Let the instrument be allowed to rotate along the z-axis. Let $\omega_a = \dot{\theta}_a$ be the rotational speed of the spacecraft about the z-axis and $\omega_b = \dot{\theta}_b$ be the rotational speed of the instrument also about the z-axis. Figure 5 illustrates the quantities required for the following development of the dynamic equations.

First note the coordinate transformation from the body coordinates of the spacecraft to the inertial coordinates

$$\begin{bmatrix} \mathbf{e}_x \\ \mathbf{e}_y \end{bmatrix} = \begin{bmatrix} \cos \theta_a & -\sin \theta_a \\ \sin \theta_a & \cos \theta_a \end{bmatrix} \begin{bmatrix} \mathbf{e}_x \\ \mathbf{e}_y \end{bmatrix} \quad (42)$$

and the transformation from the body coordinates of the instrument to the inertial coordinates

$$\begin{bmatrix} \mathbf{e}_x \\ \mathbf{e}_y \end{bmatrix} = \begin{bmatrix} \cos \theta_b & -\sin \theta_b \\ \sin \theta_b & \cos \theta_b \end{bmatrix} \begin{bmatrix} \mathbf{e}_{x'} \\ \mathbf{e}_{y'} \end{bmatrix} \quad (43)$$

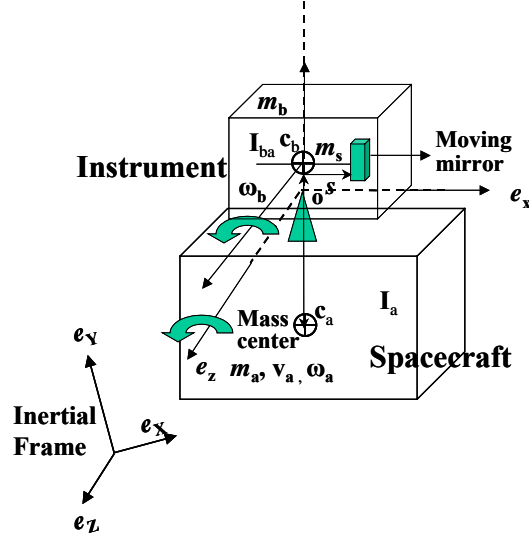


Figure 5: Body and inertia coordinates for two-rotation-axis plane motion.

The spacecraft linear momentum is

$$\begin{aligned}\mathbf{p}_a &= m_a (\mathbf{v}_a + \boldsymbol{\omega}_a \times \mathbf{c}_a) \\ &= m_a \left[(\dot{X} - c_a \cos \theta_a \dot{\theta}_a) \mathbf{e}_x + (\dot{Y} - c_a \sin \theta_a \dot{\theta}_a) \mathbf{e}_y \right]\end{aligned}\quad (44)$$

where \mathbf{v}_a is the velocity at the coordinate origin \mathbf{o} (i.e., the contact point of the spacecraft and the instrument), \dot{X} and \dot{Y} are its components along \mathbf{e}_x and \mathbf{e}_y in the inertial frame, respectively. For simplicity, without losing generality, the spacecraft center of mass \mathbf{c}_a is assumed to be in the direction of \mathbf{e}_y . The instrument linear momentum is

$$\begin{aligned}\mathbf{p}_b &= m_b [\mathbf{v}_a + \boldsymbol{\omega}_b \times \mathbf{c}_b] \\ &= m_b \left[(\dot{X} - c_b \cos \theta_b \dot{\theta}_b) \mathbf{e}_x + m_b (\dot{Y} - c_b \sin \theta_b \dot{\theta}_b) \mathbf{e}_y \right]\end{aligned}\quad (45)$$

Note that the direction of the body coordinate \mathbf{e}_y is chosen to pass through the instrument center of mass. The linear momentum of the moving-mirror traveling in the direction \mathbf{e}_x is

$$\begin{aligned}
\mathbf{p}_s &= m_s [\mathbf{v}_a + \boldsymbol{\omega}_b \times (\mathbf{c}_b + \mathbf{s}) + \dot{\mathbf{s}}] \\
&= m_s \left[\dot{X} - (c_b \cos \theta_b + s \sin \theta_b) \dot{\theta}_b + \cos \theta_b \dot{s} \right] \mathbf{e}_x \\
&\quad + m_s \left[\dot{Y} + (s \cos \theta_b - c_b \sin \theta_b) \dot{\theta}_b + \sin \theta_b \dot{s} \right] \mathbf{e}_y
\end{aligned} \tag{46}$$

Spacecraft angular momentum about the reference point \mathbf{o} is

$$\begin{aligned}
\mathbf{h}_a &= \int_{\Omega_a} \boldsymbol{\rho}_a \times [\mathbf{v}_a + \boldsymbol{\omega}_a \times \boldsymbol{\rho}_a] dm_a = m_a (\mathbf{c}_a \times \mathbf{v}_a) + \mathbf{I}_a \boldsymbol{\omega}_a \\
&= \left[-m_a c_a (\dot{X} \cos \theta_a + \dot{Y} \sin \theta_a) + \mathbf{I}_a \dot{\theta}_a \right] \mathbf{e}_z
\end{aligned} \tag{47}$$

Instrument angular momentum about the reference point \mathbf{o} is

$$\begin{aligned}
\mathbf{h}_b &= \int_{\Omega_b} \boldsymbol{\rho}_b \times [\mathbf{v}_a + \boldsymbol{\omega}_b \times \boldsymbol{\rho}_b] dm_b = m_b (\mathbf{c}_b \times \mathbf{v}_a) + \mathbf{I}_b \boldsymbol{\omega}_b \\
&= \left[-m_b c_b (\dot{X} \cos \theta_b + \dot{Y} \sin \theta_b) + \mathbf{I}_b \dot{\theta}_b \right] \mathbf{e}_z
\end{aligned} \tag{48}$$

Moving-mirror angular momentum about the reference point \mathbf{o} is

$$\begin{aligned}
\mathbf{h}_s &= m_s (\mathbf{c}_b + \mathbf{s}) \times [\mathbf{v}_a + \boldsymbol{\omega}_b \times (\mathbf{c}_b + \mathbf{s}) + \dot{\mathbf{s}}] \\
&= m_s \left\{ -(c_b \cos \theta_b + s \sin \theta_b) \dot{X} - (c_b \sin \theta_b - s \cos \theta_b) \dot{Y} + (c_b^2 + s^2) \dot{\theta}_b - c_b \dot{s} \right\} \mathbf{e}_z
\end{aligned} \tag{49}$$

To perform the parametric study, let us define the following non-dimensional quantities

$$\begin{aligned}
\bar{X} &= \frac{X}{c}; \bar{Y} = \frac{Y}{c}; \bar{s} = \frac{s}{c}; \bar{c}_a = \frac{c_a}{c}; \bar{c}_b = \frac{c_b}{c}; \\
m_1 &= \frac{m_b + m_s}{m_a + m_b + m_s}; m_2 = \frac{m_s}{m_a + m_b + m_s}; \\
\mathbf{I}_1 &= \frac{\mathbf{I}_a}{(m_a + m_b + m_s) c^2}; \mathbf{I}_2 = \frac{\mathbf{I}_b}{(m_a + m_b + m_s) c^2}
\end{aligned} \tag{50}$$

and

$$\bar{\mathbf{p}} = \frac{\mathbf{p}}{(m_a + m_b + m_s) c}; \bar{\mathbf{h}}_b + \bar{\mathbf{h}}_s = \frac{\mathbf{h}_b + \mathbf{h}_s}{(m_a + m_b + m_s) c^2}; \bar{\mathbf{h}} = \frac{\mathbf{h}}{(m_a + m_b + m_s) c^2} \tag{51}$$

where c is an arbitrary positive constant intuitively set to be $c = |c_a| + |c_b|$. Normalizing

the total linear momentum $\mathbf{p} = \mathbf{p}_a + \mathbf{p}_b + \mathbf{p}_s$ yields

$$\bar{\mathbf{p}} = \begin{bmatrix} \bar{p}_x \\ \bar{p}_y \end{bmatrix} = \begin{bmatrix} \dot{X} - (1 - m_1) \bar{c}_a \cos \theta_a \dot{\theta}_a - (m_1 \bar{c}_b \cos \theta_b + m_2 \bar{s} \sin \theta_b) \dot{\theta}_b + m_2 \dot{s} \cos \theta_b \\ \dot{Y} - (1 - m_1) \bar{c}_a \sin \theta_a \dot{\theta}_a - (m_1 \bar{c}_b \sin \theta_b - m_2 \bar{s} \cos \theta_b) \dot{\theta}_b + m_2 \dot{s} \sin \theta_b \end{bmatrix} \tag{52}$$

Normalizing the sum of the angular momentums \mathbf{h}_b and \mathbf{h}_s produces

$$\begin{aligned} \bar{\mathbf{h}}_b + \bar{\mathbf{h}}_s = & \left\{ -[m_1 \bar{c}_b \cos \theta_b + m_2 \bar{s} \sin \theta_b] \dot{\bar{X}} - [m_1 \bar{c}_b \sin \theta_b - m_2 \bar{s} \cos \theta_b] \dot{\bar{Y}} \right. \\ & \left. + [I_2 + m_2 c_b^2 + m_2 \bar{s}^2] \dot{\theta}_b - m_2 \bar{c}_b \dot{\bar{s}} \right\} \mathbf{e}_z \end{aligned} \quad (53)$$

Furthermore, normalizing the total angular momentum of the system $\mathbf{h} = \mathbf{h}_a + \mathbf{h}_b + \mathbf{h}_s$ yields

$$\begin{aligned} \bar{\mathbf{h}} = & \left\{ -[(1-m_1) \bar{c}_a \cos \theta_a + m_1 \bar{c}_b \cos \theta_b + m_2 \bar{s} \sin \theta_b] \dot{\bar{X}} \right. \\ & - [(1-m_1) \bar{c}_a \sin \theta_a + m_1 \bar{c}_b \sin \theta_b - m_2 \bar{s} \cos \theta_b] \dot{\bar{Y}} \\ & \left. + I_1 \dot{\theta}_a + [I_2 + m_2 c_b^2 + m_2 \bar{s}^2] \dot{\theta}_b - m_2 \bar{c}_b \dot{\bar{s}} \right\} \mathbf{e}_z \end{aligned} \quad (54)$$

The angular momentum in Eq. (53) or (54) has only one component along the Z axis.

Differential Equations of Motion

With no external force applied to the system and zero initial condition, differential equations of motion for the overall system translation are

$$\begin{aligned} \dot{\mathbf{p}} = \begin{bmatrix} \dot{p}_x \\ \dot{p}_y \end{bmatrix} = \begin{bmatrix} 0 \\ 0 \end{bmatrix} & \Rightarrow \dot{\bar{\mathbf{p}}} = \begin{bmatrix} \dot{\bar{p}}_x \\ \dot{\bar{p}}_y \end{bmatrix} = \begin{bmatrix} 0 \\ 0 \end{bmatrix} \\ \Rightarrow \bar{\mathbf{p}} = \begin{bmatrix} \bar{p}_x \\ \bar{p}_y \end{bmatrix} = \begin{bmatrix} \bar{p}_x(t=0) \\ \bar{p}_y(t=0) \end{bmatrix} = \begin{bmatrix} 0 \\ 0 \end{bmatrix} \end{aligned} \quad (55)$$

where $\bar{\mathbf{p}}$ is the non-dimensional quantity defined in Eq. (50) with the assumption of zero initial linear momentum, i.e., $\bar{\mathbf{P}}(t=0)=\mathbf{0}$. The differential equation for the overall system rotation with no external force and torque is

$$\dot{\mathbf{h}} = \boldsymbol{\tau} - \mathbf{v}_a \times \mathbf{p} = \mathbf{0} \Rightarrow \dot{\bar{\mathbf{h}}} = \mathbf{0} \quad (56)$$

The differential equation of motion for the instrument rotation is

$$\begin{aligned}
\dot{\mathbf{h}}_b + \dot{\mathbf{h}}_s &= -\mathbf{v}_a \times (\mathbf{p}_b + \mathbf{p}_s) + \boldsymbol{\tau}_p \\
&= -\mathbf{v}_a \times \left\{ \dot{\boldsymbol{\theta}}_b \times [(m_b + m_s)\mathbf{c}_b + m_s\mathbf{s}] + m_s\dot{\mathbf{s}} \right\} + \boldsymbol{\tau}_p \\
&= \left\{ \tau_p - m_s \dot{X} \dot{s} \sin \theta_b + m_s \dot{Y} \dot{s} \cos \theta_b \right. \\
&\quad + \dot{X} \dot{\theta}_b [-m_s s \cos \theta_b + (m_b + m_s) c_b \sin \theta_b] \\
&\quad \left. - \dot{Y} \dot{\theta}_b [m_s s \sin \theta_b + (m_b + m_s) c_b \cos \theta_b] \right\} \mathbf{e}_z
\end{aligned} \tag{57}$$

that produces the non-dimensional equation of motion

$$\begin{aligned}
\dot{\bar{\mathbf{h}}}_b + \dot{\bar{\mathbf{h}}}_s &= \left\{ \bar{\tau}_p - m_2 \dot{X} \dot{\bar{s}} \sin \theta_b + m_2 \dot{Y} \dot{\bar{s}} \cos \theta_b \right. \\
&\quad + \dot{X} \dot{\theta}_b [-m_2 \bar{s} \cos \theta_b + m_1 \bar{c}_b \sin \theta_b] \\
&\quad \left. - \dot{Y} \dot{\theta}_b [m_2 \bar{s} \sin \theta_b + m_1 \bar{c}_b \cos \theta_b] \right\} \mathbf{e}_z
\end{aligned} \tag{58}$$

where

$$\bar{\mathbf{h}}_b = \frac{\mathbf{h}_b}{(m_a + m_b + m_s)c^2}; \quad \bar{\mathbf{h}}_s = \frac{\mathbf{h}_s}{(m_a + m_b + m_s)c^2}; \quad \bar{\tau}_p = \frac{\tau_p}{(m_a + m_b + m_s)c^2} \tag{59}$$

In view of Eqs. (52), (53), and (54), the whole system can be described by the following four equations [see Eq. (15)]

$$\begin{aligned}
\dot{\bar{p}}_x &= 0; \quad \dot{\bar{p}}_y = 0; \quad \dot{\bar{h}}_z = 0; \\
\dot{\bar{h}}_z &= \bar{\tau}_p - m_2 \dot{X} \dot{\bar{s}} \sin \theta_b + m_2 \dot{Y} \dot{\bar{s}} \cos \theta_b + \dot{X} \dot{\theta}_b [-m_2 \bar{s} \cos \theta_b + m_1 \bar{c}_b \sin \theta_b] \\
&\quad - \dot{Y} \dot{\theta}_b [m_2 \bar{s} \sin \theta_b + m_1 \bar{c}_b \cos \theta_b]
\end{aligned} \tag{60}$$

where \bar{h}_z and \bar{h}_z are the components of \mathbf{h} and $\bar{\mathbf{h}}_b + \bar{\mathbf{h}}_s$ in the inertial direction \mathbf{e}_z .

Equation (60) can be integrated to solve for the time histories of \bar{p}_x , \bar{p}_y , \bar{h}_z , and \bar{h}_z .

Note that the third equation in Eq. (60) is valid only when the condition $\bar{p}_x = \bar{p}_y = 0$ is

satisfied at all times and no external torque is applied. At any time t , the quantities \dot{X} , \dot{Y} , $\dot{\theta}_a$, and $\dot{\theta}_b$ can be updated by using Eqs. (52), (53), and (54) to first form

$$\boldsymbol{\wp} = \mathbf{M} \mathbf{v} + \boldsymbol{\beta} \tag{61}$$

where

$$\wp = \begin{bmatrix} \bar{p}_x \\ \bar{p}_y \\ \bar{h}_z \\ \bar{\dot{h}}_z \end{bmatrix}; \quad \mathbf{v} = \begin{bmatrix} \dot{\bar{X}} \\ \dot{\bar{Y}} \\ \dot{\theta}_a \\ \dot{\theta}_b \end{bmatrix}; \quad \boldsymbol{\beta} = \begin{bmatrix} m_2 \dot{\bar{s}} c \theta_b \\ m_2 \dot{\bar{s}} s \theta_b \\ -m_2 \bar{c}_b \dot{\bar{s}} \\ -m_2 \bar{c}_b \dot{\bar{s}} \end{bmatrix} \quad (62)$$

and

$$\mathbf{M} = \begin{bmatrix} 1 & 0 & (m_1 - 1) \bar{c}_a c \theta_a & -m_1 \bar{c}_b c \theta_b - m_2 \bar{s} s \theta_b \\ 0 & 1 & (m_1 - 1) \bar{c}_a s \theta_a & -m_1 \bar{c}_b s \theta_b + m_2 \bar{s} c \theta_b \\ (m_1 - 1) \bar{c}_a c \theta_a & (m_1 - 1) \bar{c}_a s \theta_a & \mathbf{I}_1 & \mathbf{I}_2 + m_2 c_b^2 + m_2 \bar{s}^2 \\ -m_1 \bar{c}_b c \theta_b - m_2 \bar{s} s \theta_b & -m_1 \bar{c}_b s \theta_b + m_2 \bar{s} c \theta_b & 0 & \mathbf{I}_2 + m_2 c_b^2 + m_2 \bar{s}^2 \end{bmatrix} \quad (63)$$

yield the update equation

$$\mathbf{v} = \mathbf{M}^{-1} (\wp - \boldsymbol{\beta}) \quad (64)$$

in which

$$c \theta_a = \cos \theta_a; \quad s \theta_a = \sin \theta_a; \quad c \theta_b = \cos \theta_b; \quad s \theta_b = \sin \theta_b; \quad (65)$$

Equation (64) can then be integrated to obtain the desired quantities \bar{X} , \bar{Y} , θ_a , and θ_b

for use in computing a new quantity $\bar{\dot{h}}_z$ via integrating Eq. (60).

On the other hand, one may prefer to have a conventional set of equations of motion that involve physical accelerations. Differentiating Eqs. (52), (53), and (54) and then applying Eqs. (55), (56), and (58) produce the matrix equation of motion

$$\mathbf{M} \ddot{\mathbf{x}} = \mathbf{f} \quad (66)$$

where \mathbf{M} is defined in Eq. (63), and

$$\mathbf{x} = \begin{bmatrix} \bar{X} \\ \bar{Y} \\ \theta_a \\ \theta_b \end{bmatrix} \quad (67)$$

and

$$\mathbf{f} = \begin{bmatrix} -m_2 \ddot{s} c \theta_b + \bar{c}_a (m_1 - 1) \dot{\theta}_a^2 s \theta_a + 2m_2 \dot{s} \dot{\theta}_b s \theta_b - \dot{\theta}_b^2 (\bar{c}_b m_1 s \theta_b - m_2 \bar{s} c \theta_b) \\ -m_2 \ddot{s} s \theta_b - \bar{c}_a (m_1 - 1) \dot{\theta}_a^2 c \theta_a - 2m_2 \dot{s} \dot{\theta}_b c \theta_b + \dot{\theta}_b^2 (\bar{c}_b m_1 c \theta_b + m_2 \bar{s} s \theta_b) \\ \bar{c}_b m_2 \ddot{s} + m_2 \bar{s} \ddot{X} \dot{\theta}_b c \theta_b + \bar{c}_a (m_1 - 1) \ddot{X} \dot{\theta}_a s \theta_a - \bar{c}_a (m_1 - 1) \dot{Y} \dot{\theta}_a c \theta_a \\ -\bar{c}_b m_1 \ddot{X} \dot{\theta}_b s \theta_b + \bar{c}_b m_1 \dot{Y} \dot{\theta}_b c \theta_b - m_2 \dot{s} \left(\dot{Y} c \theta_b + 2\bar{s} \dot{\theta}_b - \ddot{X} s \theta_b \right) + \dot{Y} m_2 \bar{s} \dot{\theta}_b s \theta_b \\ \bar{\tau}_p - 2m_2 \bar{s} \dot{s} \dot{\theta}_b + c_b m_2 \ddot{s} \end{bmatrix} \quad (68)$$

What is the torque $\bar{\tau}_p$ in Eq. (68) that will drive the instrument to satisfy the precision pointing requirement? This question will be answered below.

Control Torque for Attitude Precision Pointing

The equality $\theta_b = \dot{\theta}_b = 0$ represents the condition where the instrument has no angular velocity relative to the inertial frame. The differential equations of motion for the instrument rotation with $\theta_b = \dot{\theta}_b = 0$ are

$$\begin{cases} \ddot{h}_b + \ddot{h}_s = -m_1 \bar{c}_b \ddot{X} + m_2 \bar{s} \ddot{Y} - m_2 \bar{c}_b \ddot{s} \\ \dot{h}_b + \dot{h}_s = \bar{\tau}_p + m_2 \bar{s} \dot{Y} \end{cases} \quad (69)$$

Differentiating the top equation of Eq. (69) and substituting it into the bottom equation yields the torque required for the instrument fine pointing

$$\bar{\tau}_p = -m_1 \bar{c}_b \ddot{X} + m_2 \bar{s} \ddot{Y} - m_2 \bar{c}_b \ddot{s} \quad (70)$$

where \ddot{s} is a pre-specified quantity; \ddot{X} and \ddot{Y} may be measured by using accelerometers. Equation (70) shows that the control torque is a weighted sum of the acceleration \ddot{s} for the moving mirror and the accelerations \ddot{X} and \ddot{Y} of the spacecraft at the joint with the instrument attached. Note that other control techniques, such as predictive control [12], may also be used for fine-pointing the instrument subject to known and/or unknown periodic disturbances.

For the case where the spacecraft is sufficiently large in comparison with the instrument such that

$$\ddot{X} \approx 0 \text{ and } \ddot{Y} \approx 0 \quad (71)$$

the torque shown in Eq. (70) will then approach to

$$\bar{\tau}_p \approx -m_2 \bar{c}_b \ddot{s} \quad (72)$$

System translation for $\theta_b = \dot{\theta}_b = 0$ is derived as follows. Substituting $\theta_b = \dot{\theta}_b = 0$ into Eq. (52) with the aid of Eq. (55) yields

$$\dot{\bar{X}} - (1 - m_1) \bar{c}_a \cos \theta_a \dot{\theta}_a + m_2 \dot{s} = 0 \quad (73)$$

$$\dot{\bar{Y}} - (1 - m_1) \bar{c}_a \sin \theta_a \dot{\theta}_a = 0 \quad (74)$$

From Eqs. (54) and (56), the total angular momentum for $\theta_b = \dot{\theta}_b = 0$ is

$$-[(1 - m_1) \bar{c}_a \cos \theta_a + m_1 \bar{c}_b] \dot{\bar{X}} - [(1 - m_1) \bar{c}_a \sin \theta_a - m_2 \bar{s}] \dot{\bar{Y}} + I_1 \dot{\theta}_a - m_2 \bar{c}_b \dot{s} = 0 \quad (75)$$

Equations (73), (74) and (75) produce the following differential equations to be integrated

$$\dot{\bar{X}} = \frac{-m_2 \left\{ I_1 - \bar{c}_a (1 - m_1) \left\{ \bar{c}_b \cos \theta_a + \sin \theta_a \left[-m_2 \bar{s} + (1 - m_1) \bar{c}_a \sin \theta_a \right] \right\} \right\} \dot{s}}{I_1 - (1 - m_1)^2 \bar{c}_a^2 + (1 - m_1) \bar{c}_a (m_2 \bar{s} \sin \theta_a - m_1 \bar{c}_b \cos \theta_a)} \quad (76)$$

$$\dot{\bar{Y}} = \frac{(1 - m_1)^2 m_2 \bar{c}_a (\bar{c}_b - \bar{c}_a \cos \theta_a) \sin \theta_a \dot{s}}{I_1 - (1 - m_1)^2 \bar{c}_a^2 + (1 - m_1) \bar{c}_a (m_2 \bar{s} \sin \theta_a - m_1 \bar{c}_b \cos \theta_a)} \quad (77)$$

$$\dot{\theta}_a = \frac{(1 - m_1) m_2 (\bar{c}_b - \bar{c}_a \cos \theta_a) \dot{s}}{I_1 - (1 - m_1)^2 \bar{c}_a^2 + (1 - m_1) \bar{c}_a (m_2 \bar{s} \sin \theta_a - m_1 \bar{c}_b \cos \theta_a)} \quad (78)$$

Integrating Eqs. (76), (77), and (78) simultaneously and analytically is quite difficult, if not impossible. A numerical example is given in the following section to illustrate the concept developed in this paper. In particular, we will show how the control torque works for the instrument precision pointing and its influence to other quantities such as the system translational and rotational displacements.

Parametric and Numerical Analyses

A representative case will be studied in this section. Given certain parameters, such as the mass and inertia ratios, we will derive the control torque for instrument precision pointing and show its relationship with the mirror motion and its influence to the overall system motion.

Control Torque with Given Mass and Inertia Ratios

Let us assume that the mass-center offset ratios of the spacecraft and the instrument away from the joint \mathbf{o} of the two bodies are given by.

$$\bar{c}_a = \frac{c_a}{c} = -0.9; \quad \bar{c}_b = \frac{c_b}{c} = 0.1; \quad c = |c_a| + |c_b| \quad (79)$$

where c is the total mass-center offset. In addition, assume that the mass ratios m_1 and m_2 among the spacecraft mass m_a , the instrument mass m_b , and the moving-mirror mass m_s , and the inertia ratio I_1 related to the spacecraft inertia are given as

$$\begin{aligned} m_1 &= \frac{m_b + m_s}{m_a + m_b + m_s} = 0.1; \quad m_2 = \frac{m_s}{m_a + m_b + m_s} = 0.01 \\ I_1 &= \frac{I_a}{(m_a + m_b + m_s)c^2} = 1; \quad I_2 = \frac{I_b}{(m_a + m_b + m_s)c^2} = 0.1 \end{aligned} \quad (80)$$

These ratios imply that the instrument mass plus the moving-mirror mass is 10% of the total system mass, whereas the moving-mirror mass is only 1% of the total mass. The spacecraft inertia about the point \mathbf{o} is equal to the inertia contributed by the total system mass and the total mass-center offset.

Differentiating Eqs. (76), (77), and (78) to solve for $\ddot{\bar{X}}$, $\ddot{\bar{Y}}$, and $\ddot{\theta}_a$, and substituting $\dot{\bar{X}}$, $\dot{\bar{Y}}$, and $\dot{\theta}_a$ into the resultant equation yield the control torque required for instrument precision pointing

$$\begin{aligned} \bar{\tau}_p &= \frac{[2.76705 + 0.32805(\bar{s} \sin 2\theta_a - \cos 2\theta_a)]\ddot{\bar{s}} \times 10^{-4}}{-0.3439 + 0.0081(\bar{s} \sin \theta_a - \cos \theta_a)} \\ &+ \frac{[2.25633(0.1 + 0.9 \cos \theta_a)^2(\bar{s} \cos \theta_a + \sin \theta_a)]\dot{\bar{s}}^2 \times 10^{-7}}{[-0.3439 + 0.0081(\bar{s} \sin \theta_a - \cos \theta_a)]^3} \end{aligned} \quad (81)$$

Given a mirror-motion profile such as the square wave that yields \bar{s} , $\dot{\bar{s}}$, and $\ddot{\bar{s}}$, and the spacecraft angular displacement θ_a , the control torque time history can be computed from Eq. (81). In practice, one would use Eq. (70) with the insertion of measured quantities \ddot{X} and \ddot{Y} , and pre-specified \dot{s} and \ddot{s} to compute the torque τ_p . With the control torque computed and applied to the system, the translational and rotational displacements are described by Eqs. (76), (77), and (78). For parametric analysis, let us rewrite Eqs. (76), (77), and (78) in terms of \bar{s} as the independent variable, rather than the time t , to yield

$$\frac{d\bar{X}}{d\bar{s}} = \frac{-m_2 \left\langle I_1 - \bar{c}_a(1-m_1) \left\{ \bar{c}_b \cos \theta_a + \sin \theta_a \left[-m_2 \bar{s} + (1-m_1) \bar{c}_a \sin \theta_a \right] \right\} \right\rangle}{I_1 - (1-m_1)^2 \bar{c}_a^2 + (1-m_1) \bar{c}_a (m_2 \bar{s} \sin \theta_a - m_1 \bar{c}_b \cos \theta_a)} \quad (82)$$

$$\frac{d\bar{Y}}{d\bar{s}} = \frac{(1-m_1)^2 m_2 \bar{c}_a (\bar{c}_b - \bar{c}_a \cos \theta_a) \sin \theta_a}{I_1 - (1-m_1)^2 \bar{c}_a^2 + (1-m_1) \bar{c}_a (m_2 \bar{s} \sin \theta_a - m_1 \bar{c}_b \cos \theta_a)} \quad (83)$$

$$\frac{d\theta_a}{d\bar{s}} = \frac{(1-m_1) m_2 (\bar{c}_b - \bar{c}_a \cos \theta_a)}{I_1 - (1-m_1)^2 \bar{c}_a^2 + (1-m_1) \bar{c}_a (m_2 \bar{s} \sin \theta_a - m_1 \bar{c}_b \cos \theta_a)} \quad (84)$$

Integrating Eqs. (82), (83), and (84) simultaneously for $1 \geq \bar{s} \geq 0$ produces the following three relationships, i.e., \bar{X} versus \bar{s} shown in Figure 6, \bar{y} versus \bar{s} shown in Figure 7, and θ versus \bar{s} shown in Figure 8.

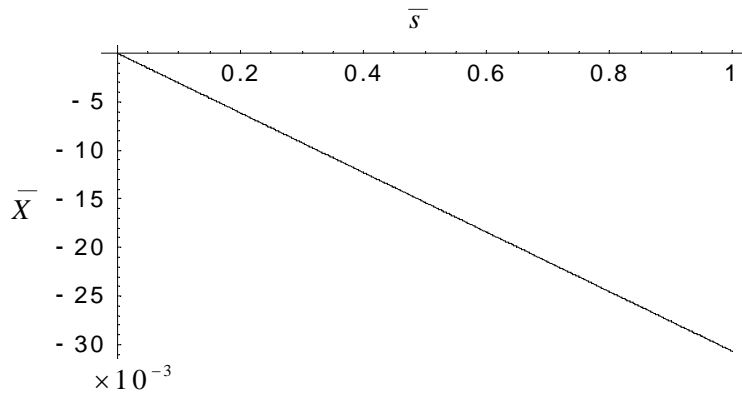


Figure 6: System displacement on X-axis versus moving-mirror displacement

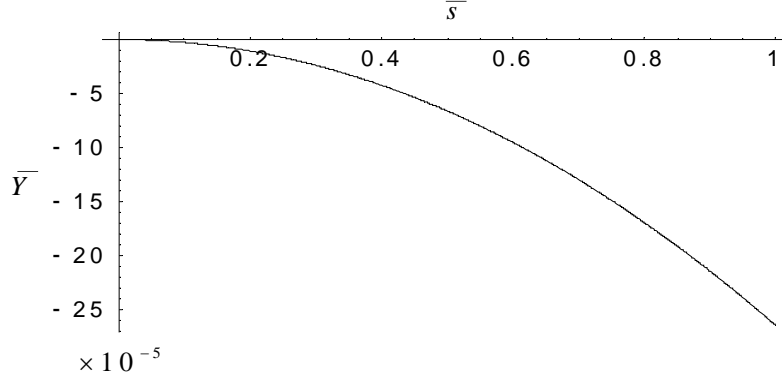


Figure 7: System displacement on Y-axis versus moving-mirror displacement

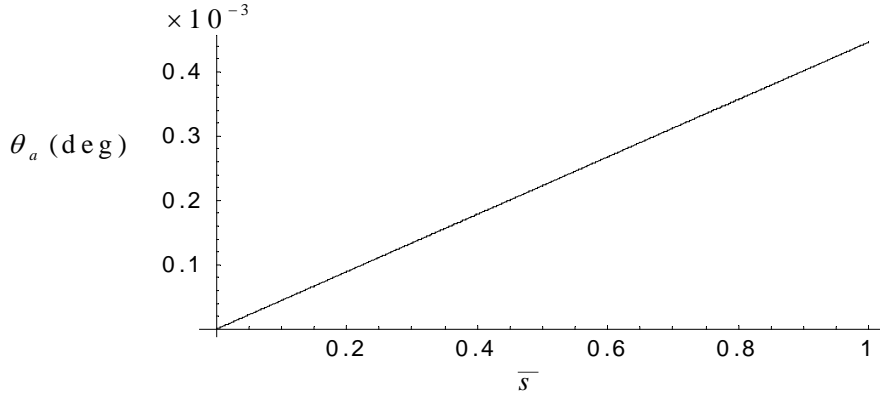


Figure 8: Angular displacement on Z-axis versus moving-mirror displacement

Observe that Figure 6 and Figure 8 show a linear relationship for small angle θ_a .

Assume that the mirror is moving as a sine wave with amplitude a and frequency ω such that

$$\begin{aligned}\bar{s} &= a \sin \omega t \\ \dot{\bar{s}} &= a\omega \cos \omega t = a\omega \sqrt{1 - \sin^2 \omega t} = a\omega \sqrt{1 - (\bar{s}/a)^2} \\ \ddot{\bar{s}} &= -a\omega^2 \sin \omega t = -\omega^2 \bar{s}\end{aligned}\tag{85}$$

Substituting Eq. (85) into Eq. (81) and plotting the result $\bar{\tau}_p$ against \bar{s} and θ_a in the range of $0.1 \geq \bar{s} \geq 0$ and $\pi/4 \geq \theta_a \geq 0$ with $\omega = 1\text{Hz}$ yields Figure 9, showing that large amplitude \bar{s} and displacement θ_a will require higher torque $\bar{\tau}_p$ for fine-pointing control.

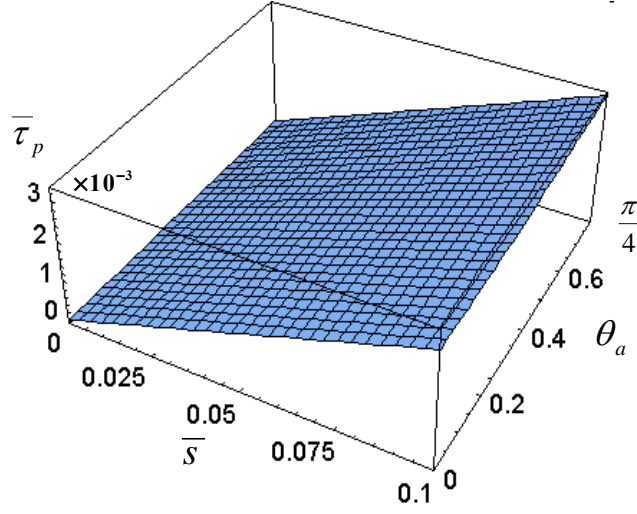


Figure 9: Control torque $\bar{\tau}_p$ versus moving-mirror displacement \bar{s} and spacecraft angular displacement θ_a

Control Torque for $\theta_a = 0$

Consider another case where $\theta_a = 0$. System equations (76), (77), and (78) for linear and angular velocities become

$$\begin{bmatrix} \dot{\bar{X}} \\ \dot{\bar{Y}} \\ \dot{\theta}_a \end{bmatrix} = \frac{1}{\gamma} \begin{bmatrix} -m_2 [\mathbf{I}_1 - \bar{c}_a \bar{c}_b (1 - m_1)] \dot{\bar{s}} \\ 0 \\ (1 - m_1) m_2 (\bar{c}_b - \bar{c}_a) \dot{\bar{s}} \end{bmatrix}; \quad \gamma = \mathbf{I}_1 - (1 - m_1)^2 \bar{c}_a^2 - (1 - m_1) \bar{c}_a \bar{c}_b m_1 \quad (86)$$

Differentiating Eqs. (76), (77), and (78) to solve for $\ddot{\bar{X}}$, $\ddot{\bar{Y}}$, and $\ddot{\theta}_a$ with $\theta_a = 0$ for linear and angular accelerations yields

$$\begin{bmatrix} \ddot{\bar{X}} \\ \ddot{\bar{Y}} \\ \ddot{\theta}_a \end{bmatrix} = \begin{bmatrix} -\frac{m_2 [\mathbf{I}_1 - \bar{c}_a \bar{c}_b (1 - m_1)] \ddot{\bar{s}}}{\gamma} - \frac{\bar{c}_a^2 (1 - m_1)^4 m_2^3 (\bar{c}_a - \bar{c}_b)^2 \dot{\bar{s}}^2}{\gamma^3} \\ \frac{\bar{c}_a (1 - m_1)^3 m_2^2 (\bar{c}_b - \bar{c}_a)^2 \dot{\bar{s}}^2}{\gamma^2} \\ \frac{(1 - m_1) m_2 (\bar{c}_b - \bar{c}_a) \ddot{\bar{s}}}{\gamma} - \frac{\bar{c}_a (1 - m_1)^3 m_2^3 (\bar{c}_a - \bar{c}_b)^2 \dot{\bar{s}}^2}{\gamma^3} \end{bmatrix} \quad (87)$$

The control torque for inertia pointing when $\theta_a = 0$ becomes

$$\begin{aligned}\bar{\tau}_p &= -m_1 \bar{c}_b \ddot{\bar{X}} + m_2 \bar{s} \ddot{\bar{Y}} - m_2 \bar{c}_b \ddot{\bar{s}} \\ &= -\frac{\bar{c}_b [\bar{I}_1 - \bar{c}_a^2 (1 - m_1)] (1 - m_1) m_2 \ddot{\bar{s}}}{\bar{I}_1 - (1 - m_1)^2 \bar{c}_a^2 - (1 - m_1) \bar{c}_a \bar{c}_b m_1} \\ &\quad + \frac{\bar{c}_a (\bar{c}_a - \bar{c}_b)^2 [\bar{I}_1 - \bar{c}_a^2 (1 - m_1)^2] (1 - m_1)^3 m_2^3 \dot{\bar{s}}^2}{[\bar{I}_1 - (1 - m_1)^2 \bar{c}_a^2 - (1 - m_1) \bar{c}_a \bar{c}_b m_1]^3}\end{aligned}\quad (88)$$

Equation (88) implies that the control torque $\bar{\tau}_p$ can be expressed in terms of \bar{s} , $\dot{\bar{s}}$, and $\ddot{\bar{s}}$ at any given angle θ_a , because the linear accelerations $\ddot{\bar{X}}$ and $\ddot{\bar{Y}}$ are purely induced by the mirror motion with the absence of external forces. Inserting the numerical values shown in Eqs. (79) and (80) into Eqs. (86), (87), and (88) yields

$$\begin{bmatrix} \dot{\bar{X}} \\ \dot{\bar{Y}} \\ \dot{\theta}_a \end{bmatrix} = \begin{bmatrix} -3.07102 \times 10^{-2} \dot{\bar{s}} \\ 0 \\ 2.55682 \times 10^{-2} \dot{\bar{s}} \end{bmatrix} \quad (89)$$

$$\begin{bmatrix} \ddot{\bar{X}} \\ \ddot{\bar{Y}} \\ \ddot{\theta}_a \end{bmatrix} = \begin{bmatrix} -3.07102 \times 10^{-2} \ddot{\bar{s}} - 1.2185 \times 10^{-5} \bar{s} \dot{\bar{s}}^2 \\ -5.29523 \times 10^{-4} \dot{\bar{s}}^2 \\ 2.55682 \times 10^{-2} \ddot{\bar{s}} + 1.50433 \times 10^{-5} \bar{s} \dot{\bar{s}}^2 \end{bmatrix} \quad (90)$$

and

$$\bar{\tau}_p = -6.92898 \times 10^{-4} \ddot{\bar{s}} - 5.17388 \times 10^{-6} \bar{s} \dot{\bar{s}}^2 \quad (91)$$

It is clear that the acceleration $\ddot{\bar{s}}$ dominates the dependent quantities to be computed in Eqs. (90) and (91).

Numerical Simulation

Assume that the moving-mirror is traveling as a sine wave such that

$$\bar{s} = a(1 - \cos \omega t); \quad \dot{\bar{s}} = a\omega \sin \omega t; \quad \ddot{\bar{s}} = a\omega^2 \cos \omega t \quad (92)$$

Let the amplitude a and the traveling frequency ω be

$$a = 0.1; \quad \omega = 1 \text{ Hz} \quad (93)$$

Integrating Eq. (66) with the insertion of numerical values defined in Eqs. (79) and (80) and zero initial condition generates the time histories for \bar{X} , \bar{Y} , θ_a , and θ_b shown in Figure 10 and for $\dot{\bar{X}}$, $\dot{\bar{Y}}$, $\dot{\theta}_a$, and $\dot{\theta}_b$ shown in Figure 11. The control-torque time histories are given in Figure 12. The curves marked in red in Figure 10 through Figure 12 show the time histories with no control torque. The curves in green give the time histories with partial control feedback only from the acceleration \ddot{s} of the mirror motion [see Eq. (72)]. The curves in blue represent the time histories with full-control feedback as defined in Eq. (70) from the acceleration \ddot{s} , and the accelerations $\ddot{\bar{X}}$ and $\ddot{\bar{Y}}$ of the spacecraft at the joint with the instrument attached.

Intuitively, we may consider only the feedback of the original acceleration source, i.e., \ddot{s} due to the mirror motion, and ignore other accelerations induced by the source. The time history in green for the pointing error θ_b shown in Figure 12 illustrates a clear reduction with control half that of the time history in red without control. Nevertheless, it is seen from the lower part of Figure 12 that the control torque, marked in green, with the absence of $\ddot{\bar{X}}$ and $\ddot{\bar{Y}}$ feedback expresses an overshoot in magnitude relative to the full-control torque in blue. It reflects the displacement overshoot, i.e., from positive displacement in red without control (cross the blue line on the zero axis) to become negative displacement in green with mirror acceleration control only. With full control including \ddot{s} , $\ddot{\bar{X}}$, and $\ddot{\bar{Y}}$ feedback, the pointing error θ_b marked in blue vanishes completely.

The time histories for the system displacement \bar{X} with and without control are approximately two orders in magnitude larger than those for the displacement \bar{Y} . The same statement is also true for the velocity time histories. This is due to the fact that the simulation begins with the angle at $\theta_a = 0$ and the mirror motion initially perpendicular to the Y axis. In addition, since the instrument including the moving mirror is much smaller in weight and inertia than the spacecraft, the control torque required for the instrument pointing does not induce much into the spacecraft rotation angle θ_a and its

angular velocity $\dot{\theta}_a$. As a result, the control torque would influence the X-axis motion much more than the Y-axis motion.

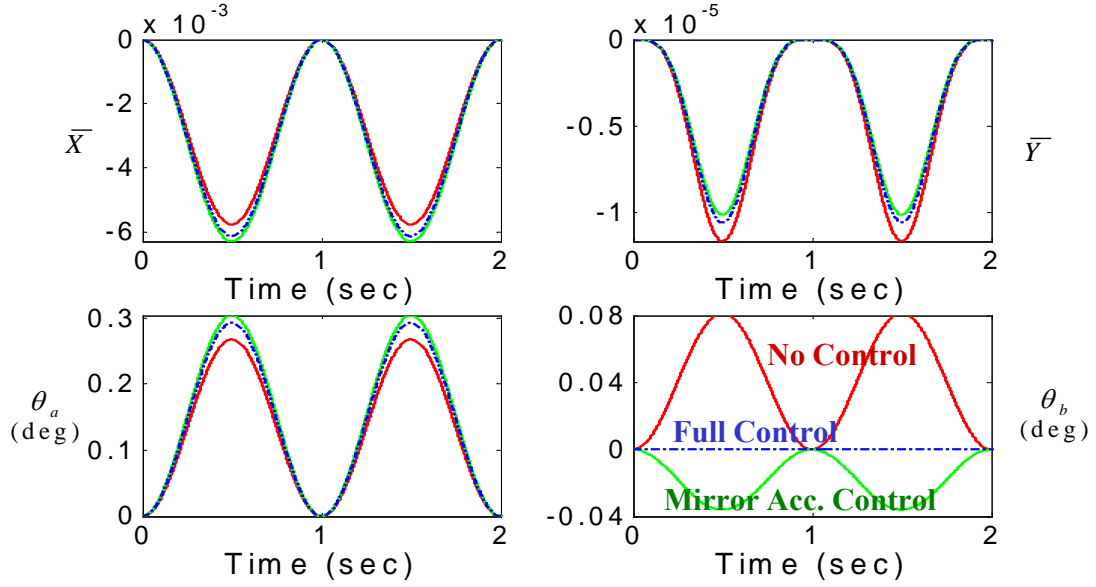


Figure 10: Time histories for \bar{X} , \bar{Y} , θ_a , and θ_b with and without control torque

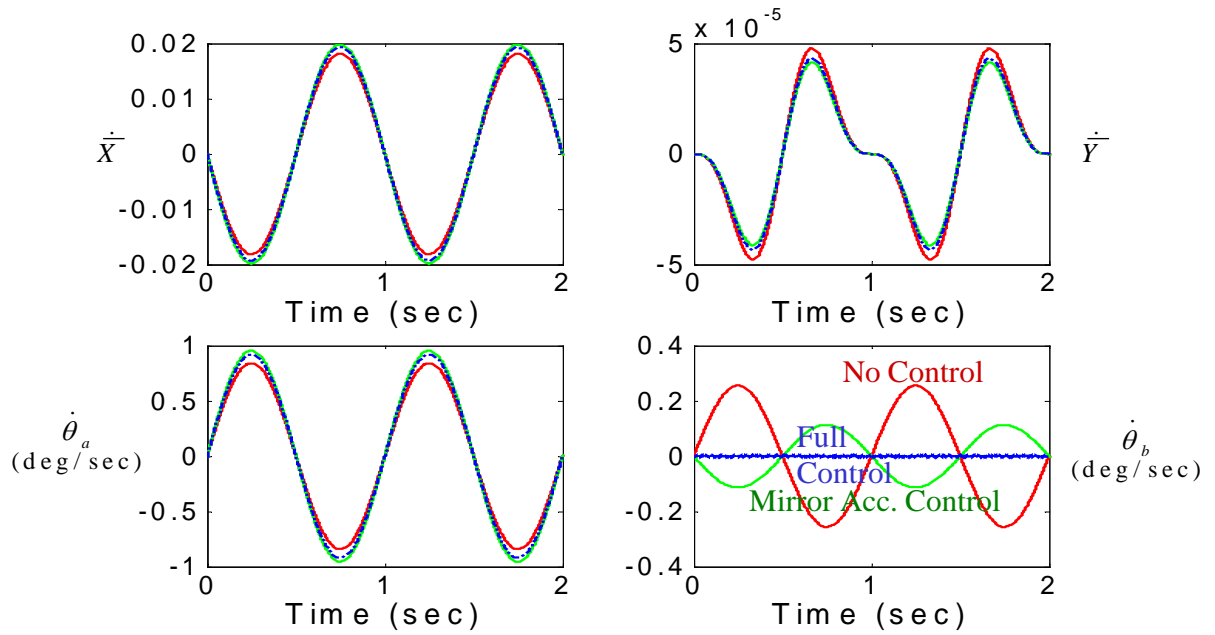


Figure 11: Time histories for $\dot{\bar{X}}$, $\dot{\bar{Y}}$, $\dot{\theta}_a$, and $\dot{\theta}_b$ with and without control torque

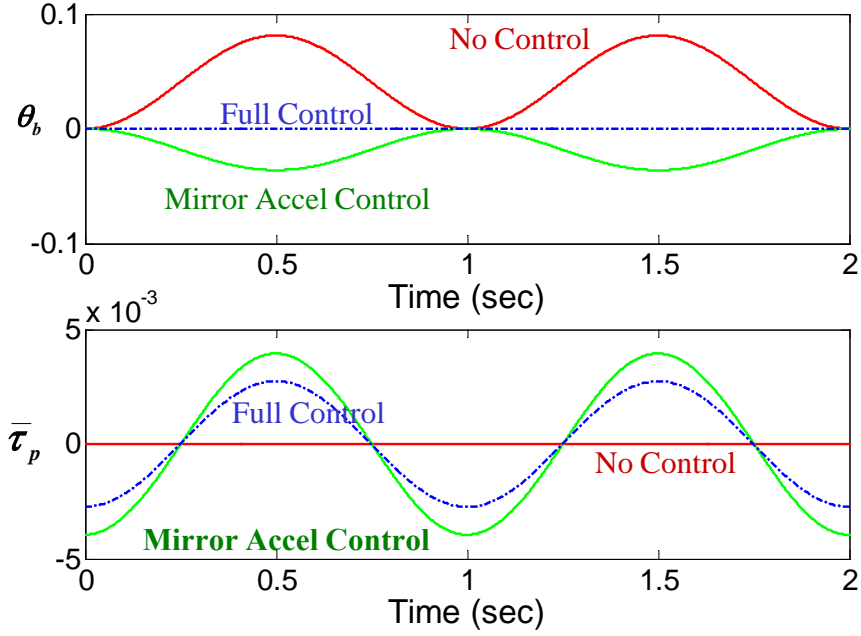


Figure 12: Time histories for pointing error θ_b and control torque $\bar{\tau}_p$.

Concluding Remarks

Parametric and numerical studies are performed in this paper to analyze attitude precision dynamics and control for an instrument gimbaled to a spacecraft. We focus on the attitude pointing error caused by the internal disturbance from a moving mirror inside the instrument. First, we examine the relationship among the pointing angle error, the inertia ratio, and the moving-mirror displacement, assuming that the instrument is locked to the spacecraft. An analytical solution is derived for the complex, but very useful, relationship that provides a road map for an engineer to determine how to design an optimal configuration for an instrument with a moving mirror. Secondly, we examine the case when active control is needed to counter balance or reject the internal disturbance for attitude precision control. A simple control law is developed producing the control torque that is capable of eliminating the pointing error induced by the internal disturbance. The control torque is a weighted sum of the mirror moving acceleration and the system linear acceleration at the point where the instrument is attached to the spacecraft. A

system/control engineer may minimize the control torque by reducing the weighting coefficients that mainly depend on the instrument configuration. Note that all analytical solutions in this paper are derived under the assumption of single rotation axis. The concept and approach are believed to be applicable to general cases. Numerical results from a sample case indicate the importance of an appropriate control torque otherwise overshoot may occur that, in turn, waste the control energy.

References

1. Smith, W., Harrison, F., Hinton, D., Miller, J., Blythe, M., Zhou, D., Revercomb, H., Best, F., Huang, H., Knuteson, R., Tobin, D., Velden, C., Bingham, G., Huppi, R., Thurgood, A., Zollinger, L., Esplin, R., and Petersen, R., "The Geosynchronous Imaging Fourier Transform Spectrometer (GIFTS): In *Conference on Satellite Meteorology and Oceanography*, 11th, Madison, WI, 15-18 October 2001. Boston, American Meteorological Society, 2001, pp700-707.
2. Singla, P., Griffith, T., and Junkins, J.L., "Determination and Autonomous On-Orbit Calibration of Star Tracker for the GIFTS Mission," *2001 Core Technologies for Space Systems Conference*, Colorado Springs, CO, November 28-30, 2001.
3. Griffith, D.T., Singla, P., Junkins, J.L., "Autonomous On-orbit Calibration Approaches for Star Tracker Cameras," *AAS/ AIAA Space Flight Mechanics Meeting*, Paper No. AAS 02-102, San Antonio, TX, January 27-30, 2002.
4. Singla, P., Griffith, T.D., Crassidis, J.L., Junkins, J.L., "Attitude Determination and Autonomous On-Orbit Calibration of Star Tracker for the GIFTS Mission," Paper No. AAS 02-101, *AAS/ AIAA Space Flight Mechanics Meeting* , San Antonio, TX, January 27-30, 2002.
5. Samaan, M.A., Mortari, D., Pollock, T.C., and Junkins, J.L., "Predictive Centroiding for Single and Multiple FOVs Star Trackers," Paper AAS 02-103, San Antonio, TX, Jan 27-30, 2002, *Journal of the Astronautical Sciences*, Vol. 50, No. 1, pp. 113-123, Janu-March 2002.

6. Kim, H-Y., and Junkins, J.L., "Self Organizing Guide Star Selection Algorithm for Ref. 7 Star Trackers: Thinning Method," *2002 IEEE Aerospace Conference*, Big Sky Montana, March 9-16, 2002.
8. Juang, J.-N., Kim, H. Y., and Junkins, J. L., "An Efficient And Robust Singular Value Method for Star Pattern Recognition and Attitude Determination", *NASA/TM-2003-212142*, January 2003, pp. 1-22.
9. Singla, P. Crassidis, J.L., and Junkins, J.L., "Spacecraft Angular Rate Estimation Algorithms for a Star Tracker Mission," Paper No. AAS 03-191, *13th Annual AAS/AIAA Space Flight Mechanics Meeting*, Ponce, Puerto Rico, Feb. 9-13, 2003.
10. Samaan, M.A., Mortari, D., and Junkins, J.L., "Non Dimensional Star Identification for Uncalibrated Star Cameras," Paper No. AAS 03-131, *13th Annual AAS/AIAA Space Flight Mechanics Meeting*, Ponce, Puerto Rico, Feb. 9-13, 2003.
11. Hughes, P. C., *Spacecraft Attitude Dynamics*, John Wiley & Sons, New York, 1986, pp. 39-83
12. Juang, J-N. and Phan, M. Q., *Identification and Control of Mechanical Systems*, Cambridge University Press, New York, 2001

REPORT DOCUMENTATION PAGE					Form Approved OMB No. 0704-0188	
<p>The public reporting burden for this collection of information is estimated to average 1 hour per response, including the time for reviewing instructions, searching existing data sources, gathering and maintaining the data needed, and completing and reviewing the collection of information. Send comments regarding this burden estimate or any other aspect of this collection of information, including suggestions for reducing this burden, to Department of Defense, Washington Headquarters Services, Directorate for Information Operations and Reports (0704-0188), 1215 Jefferson Davis Highway, Suite 1204, Arlington, VA 22202-4302. Respondents should be aware that notwithstanding any other provision of law, no person shall be subject to any penalty for failing to comply with a collection of information if it does not display a currently valid OMB control number.</p> <p>PLEASE DO NOT RETURN YOUR FORM TO THE ABOVE ADDRESS.</p>						
1. REPORT DATE (DD-MM-YYYY)		2. REPORT TYPE			3. DATES COVERED (From - To)	
01- 08 - 2004		Technical Memorandum				
4. TITLE AND SUBTITLE Instrument Attitude Precision Control				5a. CONTRACT NUMBER		
				5b. GRANT NUMBER		
				5c. PROGRAM ELEMENT NUMBER		
6. AUTHOR(S) Juang, Jer-Nan				5d. PROJECT NUMBER		
				5e. TASK NUMBER		
				5f. WORK UNIT NUMBER 23-873-00-2B		
7. PERFORMING ORGANIZATION NAME(S) AND ADDRESS(ES) NASA Langley Research Center Hampton, VA 23681-2199				8. PERFORMING ORGANIZATION REPORT NUMBER L-19042		
9. SPONSORING/MONITORING AGENCY NAME(S) AND ADDRESS(ES) National Aeronautics and Space Administration Washington, DC 20546-0001				10. SPONSOR/MONITOR'S ACRONYM(S) NASA		
				11. SPONSOR/MONITOR'S REPORT NUMBER(S) NASA/TM-2004-213251		
12. DISTRIBUTION/AVAILABILITY STATEMENT Unclassified - Unlimited Subject Category 39 Availability: NASA CASI (301) 621-0390 Distribution: Standard						
13. SUPPLEMENTARY NOTES An electronic version can be found at http://techreports.larc.nasa.gov/ltrs/ or http://ntrs.nasa.gov						
14. ABSTRACT A novel approach is presented in this paper to analyze attitude precision and control for an instrument gimbaled to a spacecraft subject to an internal disturbance caused by a moving component inside the instrument. Nonlinear differential equations of motion for some sample cases are derived and solved analytically to gain insight in examining the influence of the disturbance to the attitude pointing error. A simple control law is developed to eliminate the instrument pointing error caused by the internal disturbance. Several cases are presented to demonstrate and verify the concept presented in this paper.						
15. SUBJECT TERMS Attitude dynamics and control; Feedback control; Spacecraft dynamics						
16. SECURITY CLASSIFICATION OF:			17. LIMITATION OF ABSTRACT	18. NUMBER OF PAGES	19a. NAME OF RESPONSIBLE PERSON	
a. REPORT	b. ABSTRACT	c. THIS PAGE			STI Help Desk (email: help@sti.nasa.gov)	
U	U	U	UU	35	19b. TELEPHONE NUMBER (Include area code) (301) 621-0390	